

# Sandbox Results

March 6, 2012

## 1 The only Flux plot(s)

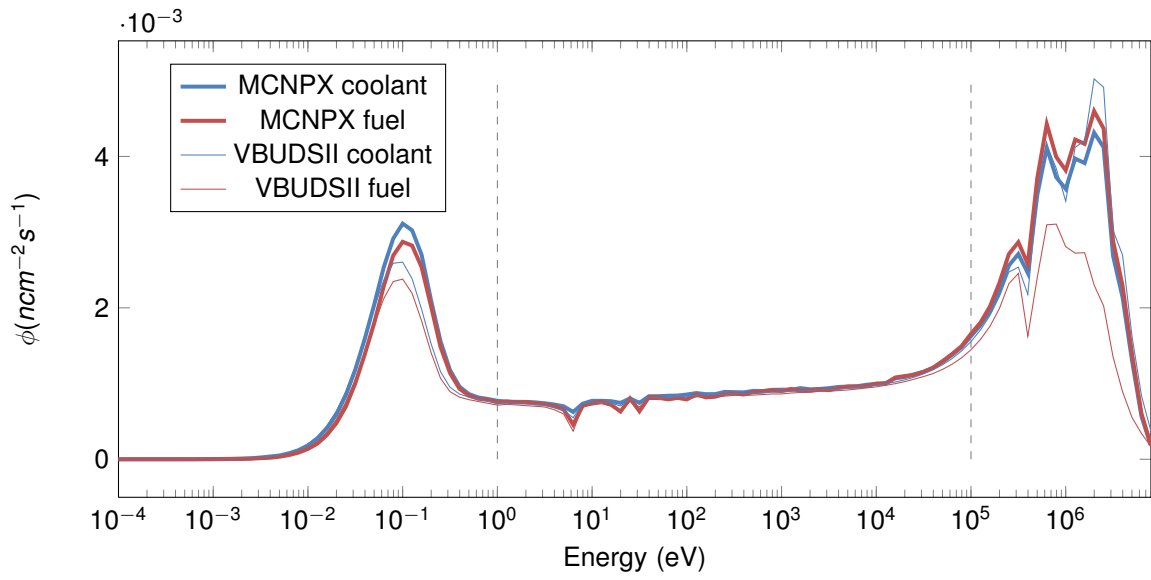


Figure 1: Energy dependent flux in both cells of the reactor, generated by MCNPX and VBUDSII.

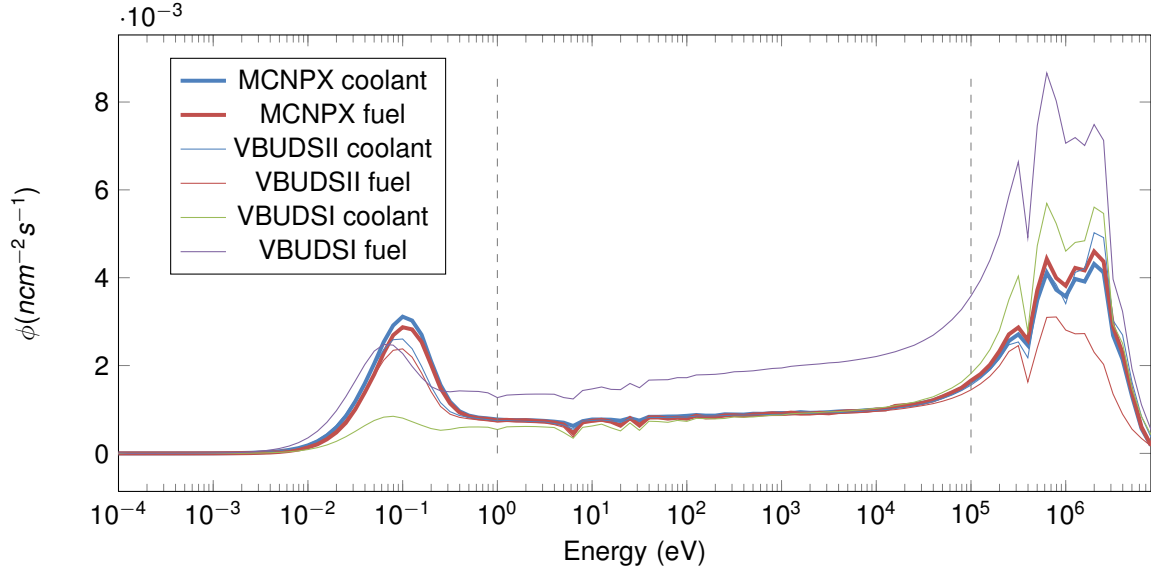


Figure 2: Energy dependent flux in both cells of the reactor, generated by MCNPX, VBUDSII and VBUDSI.

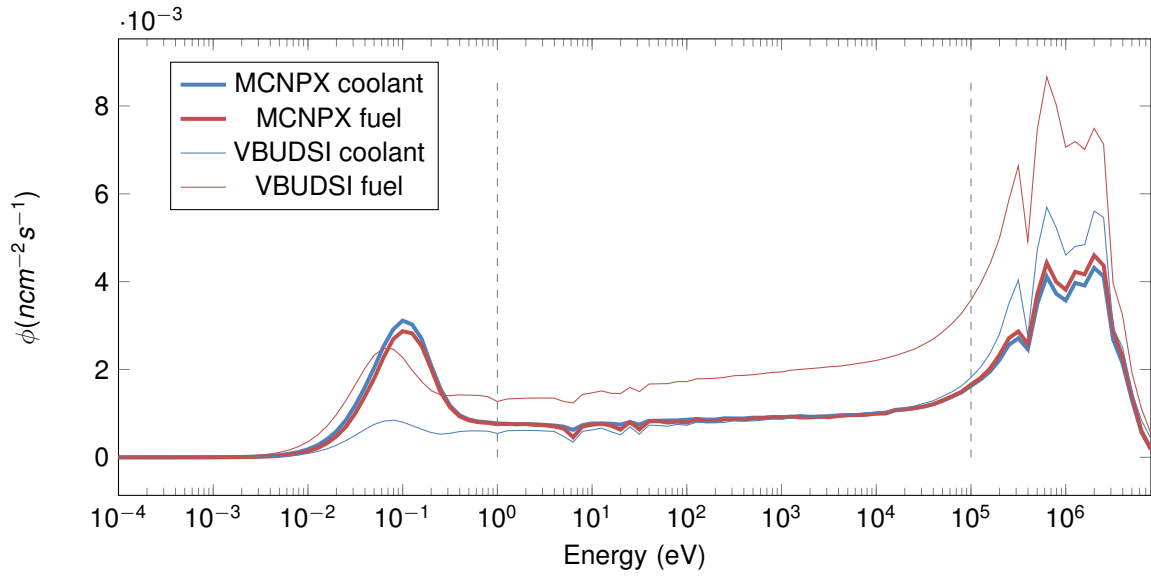


Figure 3: Energy dependent flux in both cells of the reactor, generated by MCNPX and VBUDSI.

## 1.1 Cross sections in cell H2O

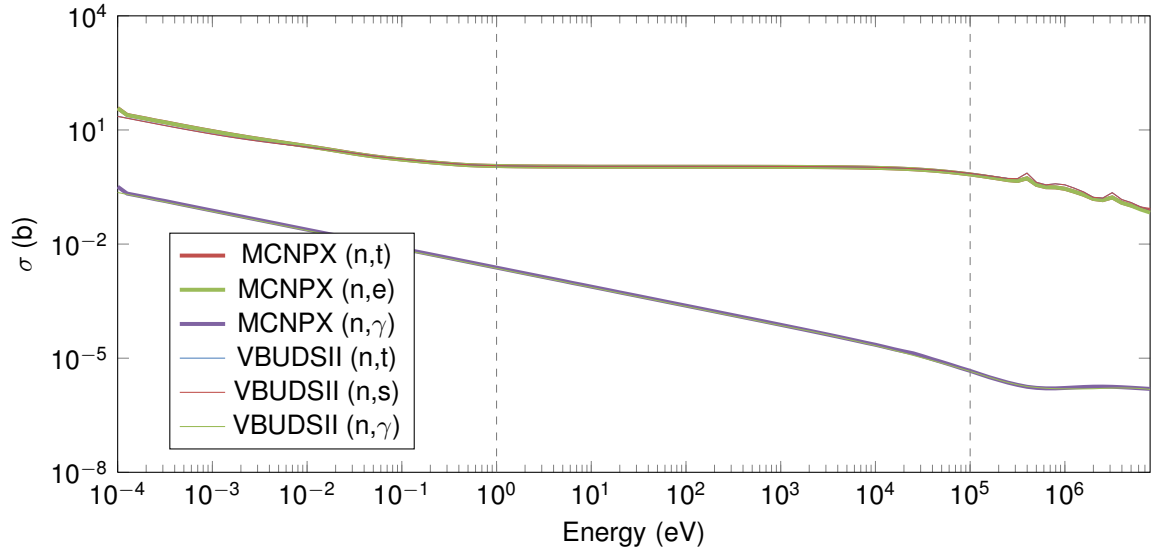


Figure 4: Energy-dependent cross sections for the H2O cell, generated by VBUDSII.

### 1.1.1 Cross sections in cell H2O, for ZAID 222

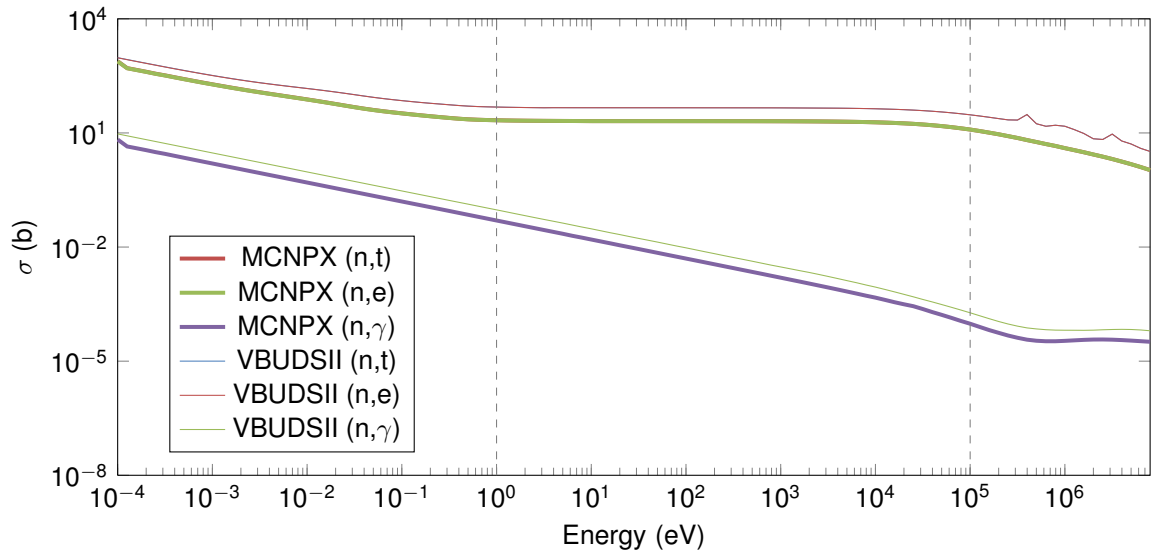


Figure 5: Energy-dependent cross sections in the H2O cell for ZAID 222, generated by both MCNPX and VBUDSII.

### 1.1.2 Cross sections in cell H2O, for ZAID 222, separated by reaction type

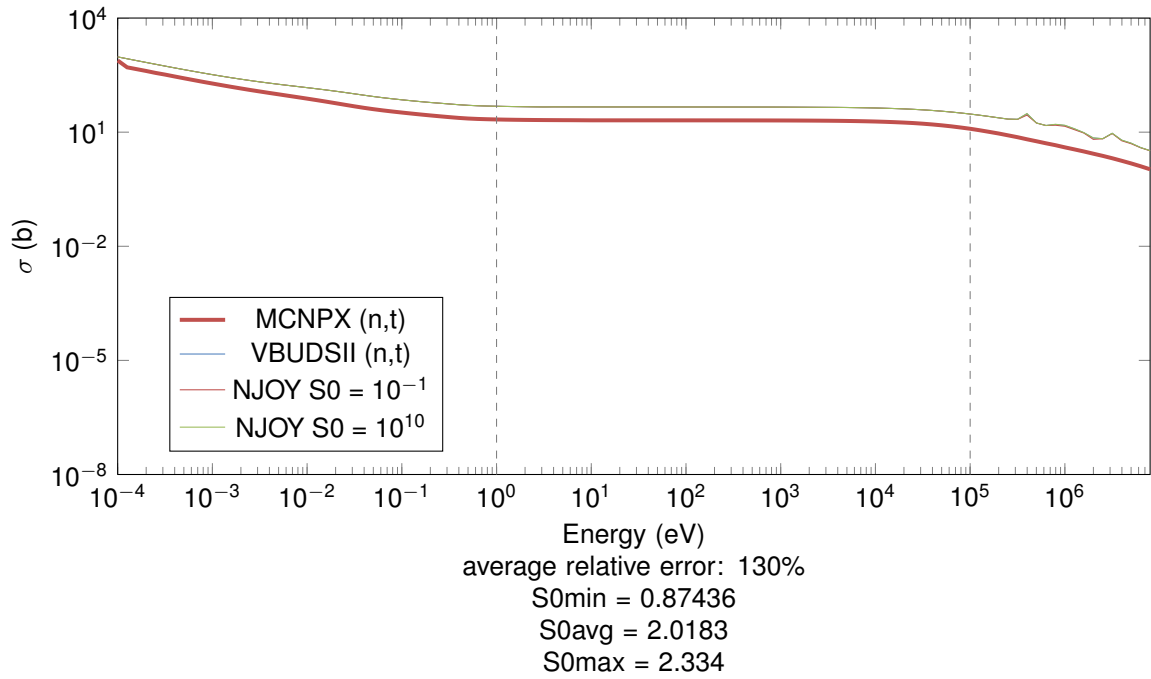


Figure 6: Energy-dependent cross sections in the H2O cell for ZAID 222 and MT 7, generated by both MCNPX and VBUDSII.

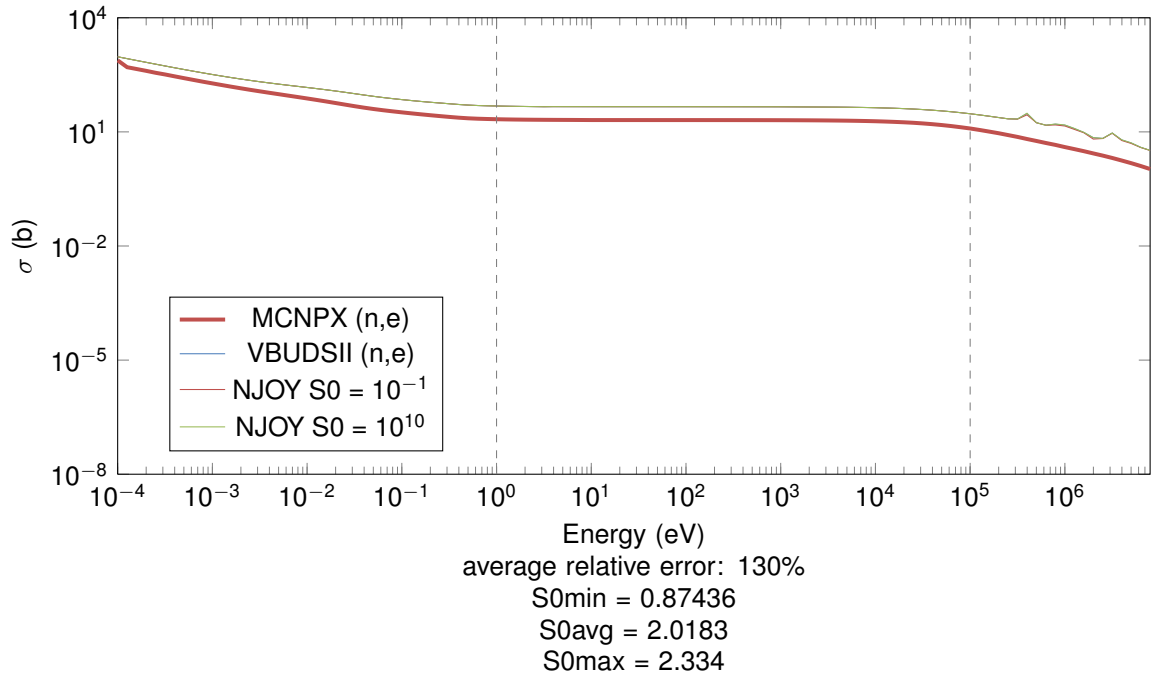


Figure 7: Energy-dependent cross sections in the H2O cell for ZAID 222 and MT 2, generated by both MCNPX and VBUDSII.

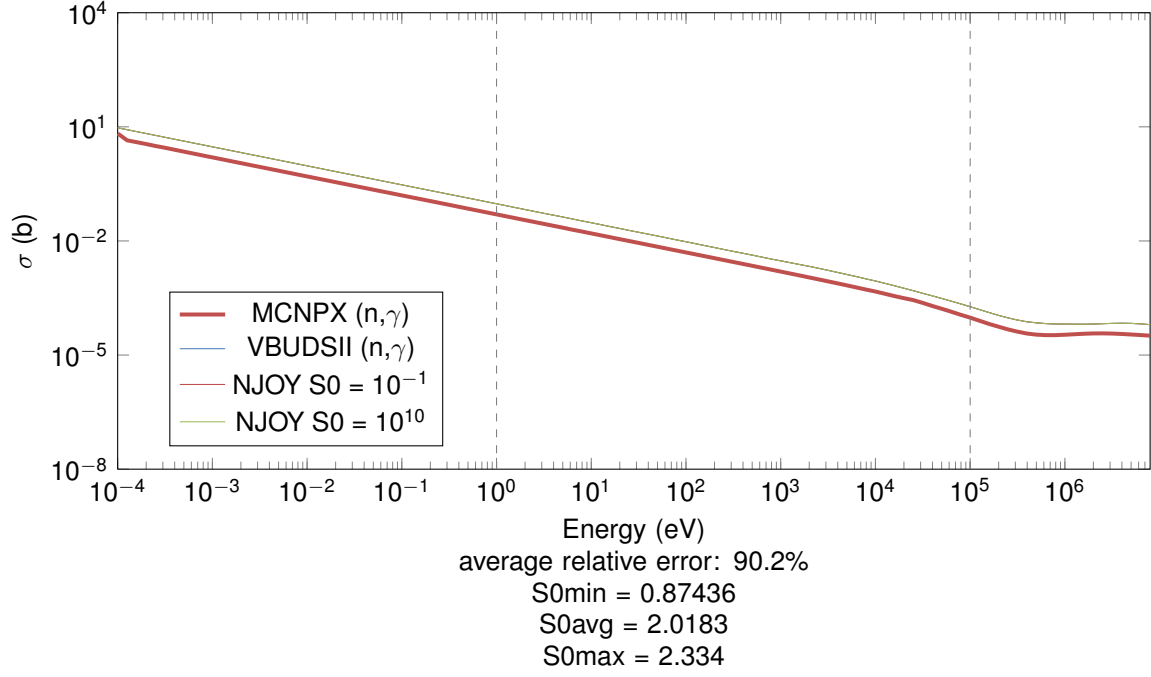


Figure 8: Energy-dependent cross sections in the H<sub>2</sub>O cell for ZAID 222 and MT 102, generated by both MCNPX and VBUDSII.

## 1.2 Cross sections in cell UO2

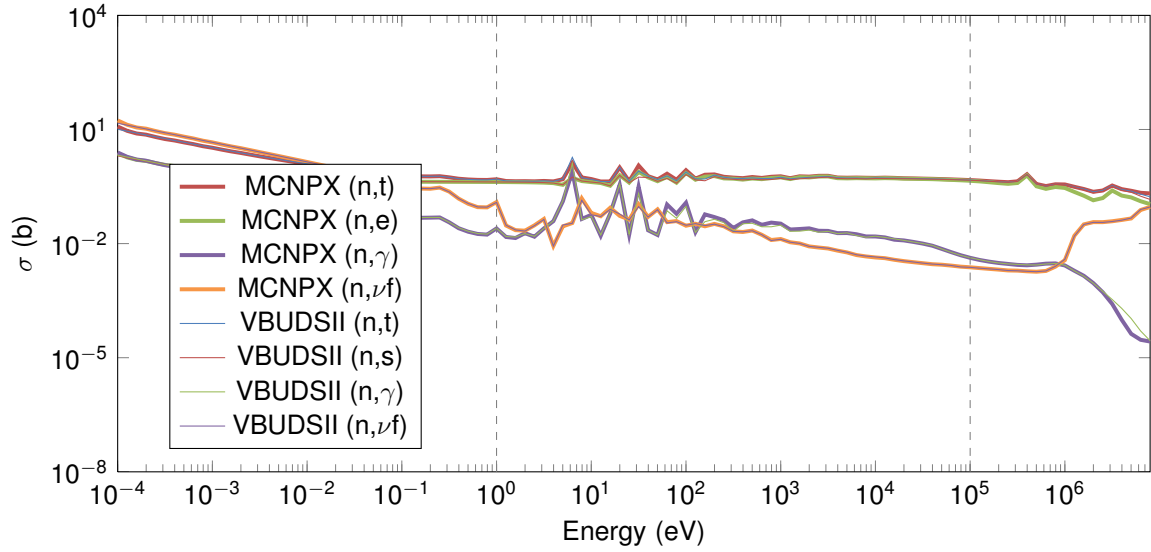


Figure 9: Energy-dependent cross sections for the UO<sub>2</sub> cell, generated by VBUDSII.

### 1.2.1 Cross sections in cell UO2, for ZAID 92235

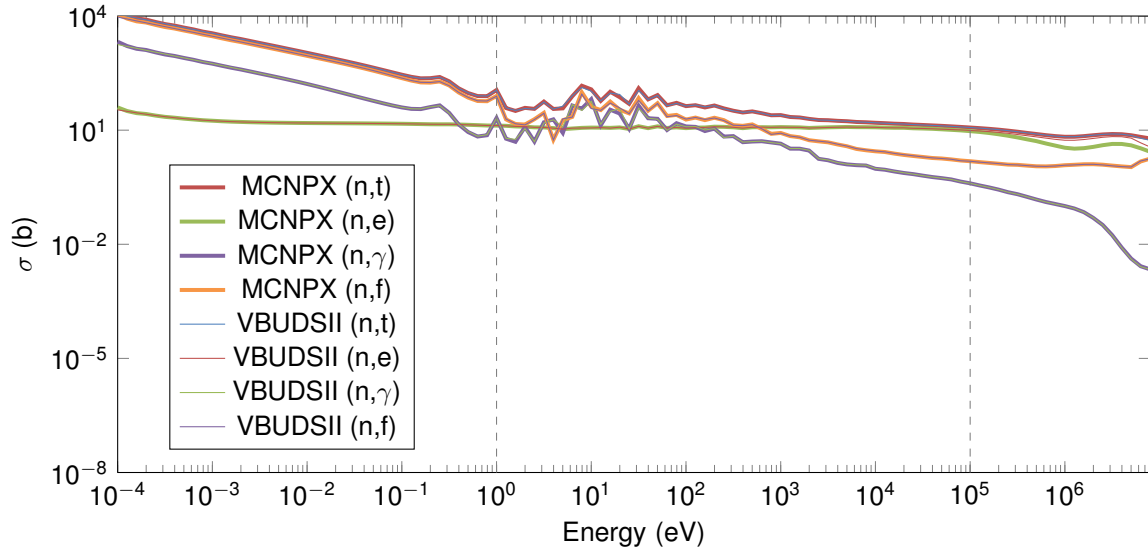


Figure 10: Energy-dependent cross sections in the UO2 cell for ZAID 92235, generated by both MCNPX and VBUDSII.

### 1.2.2 Cross sections in cell UO2, for ZAID 92235, separated by reaction type

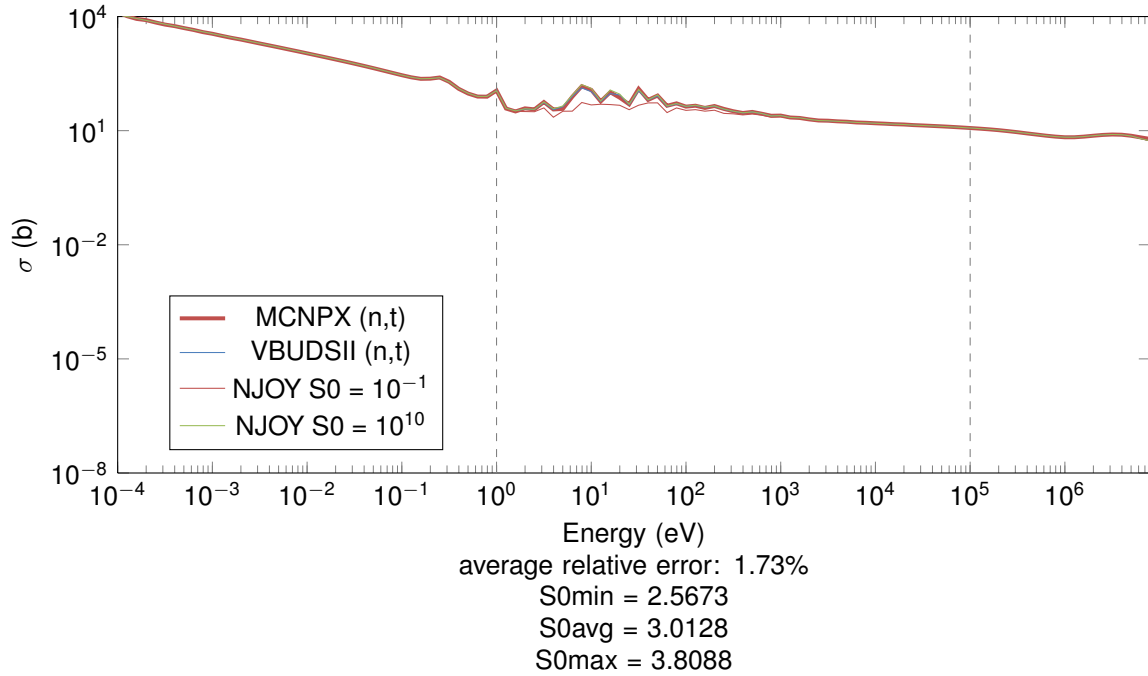


Figure 11: Energy-dependent cross sections in the UO2 cell for ZAID 92235 and MT 7, generated by both MCNPX and VBUDSII.

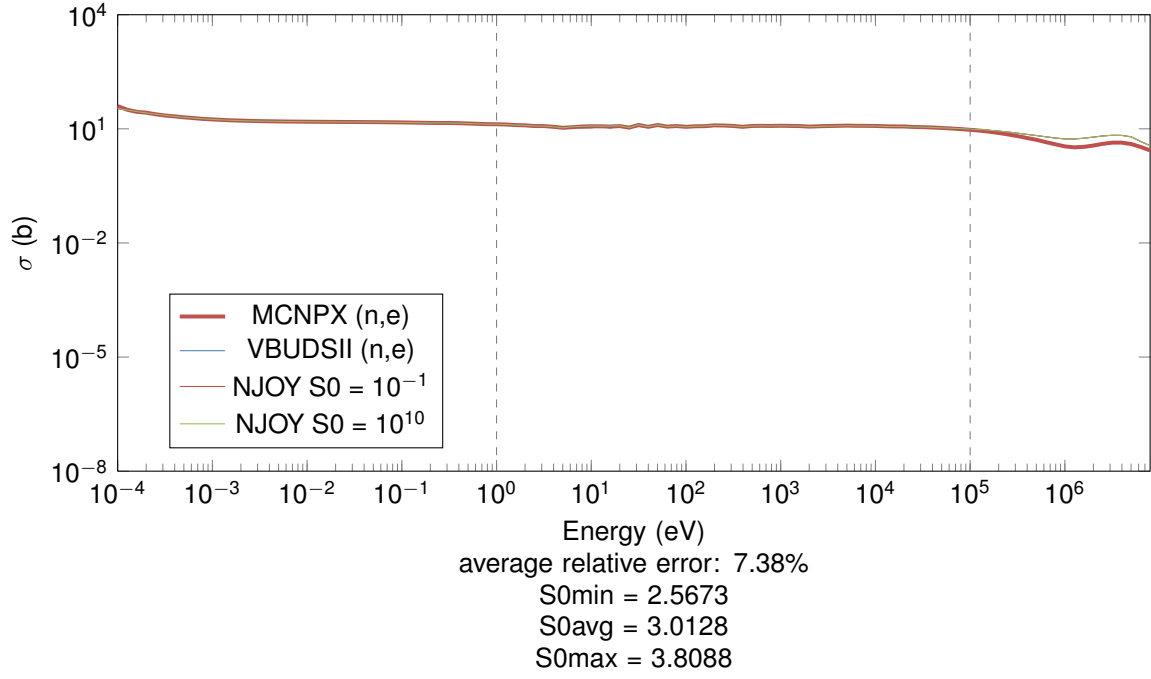


Figure 12: Energy-dependent cross sections in the UO2 cell for ZAIID 92235 and MT 2, generated by both MCNPX and VBUDSII.

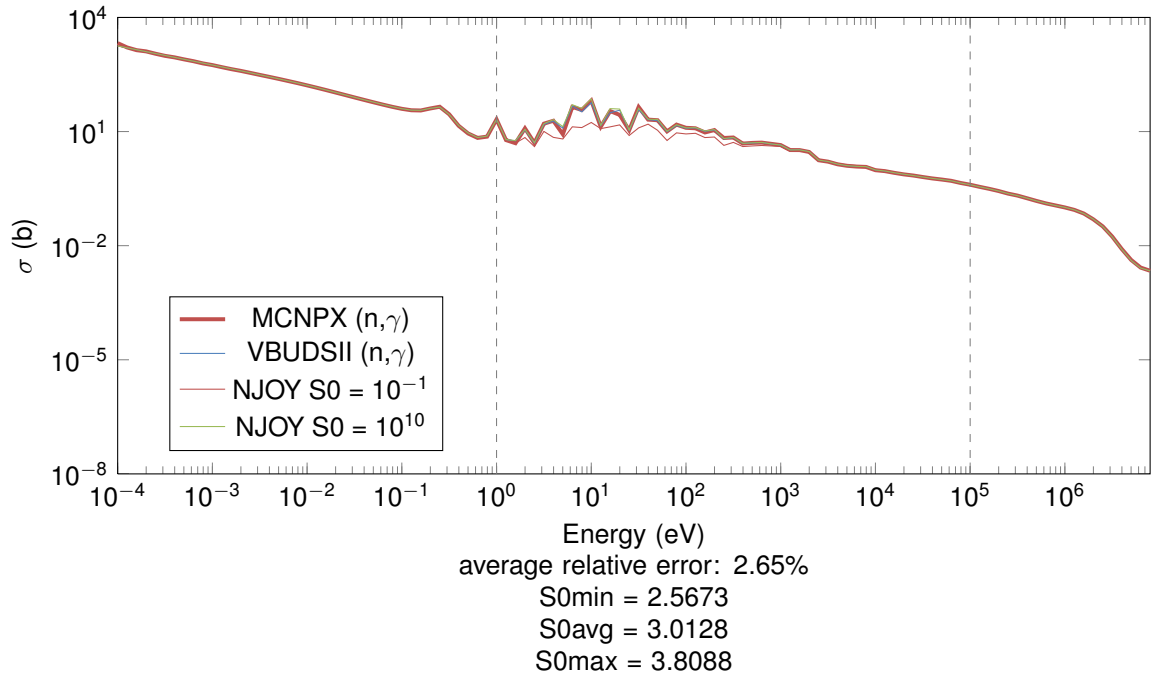


Figure 13: Energy-dependent cross sections in the UO2 cell for ZAIID 92235 and MT 102, generated by both MCNPX and VBUDSII.

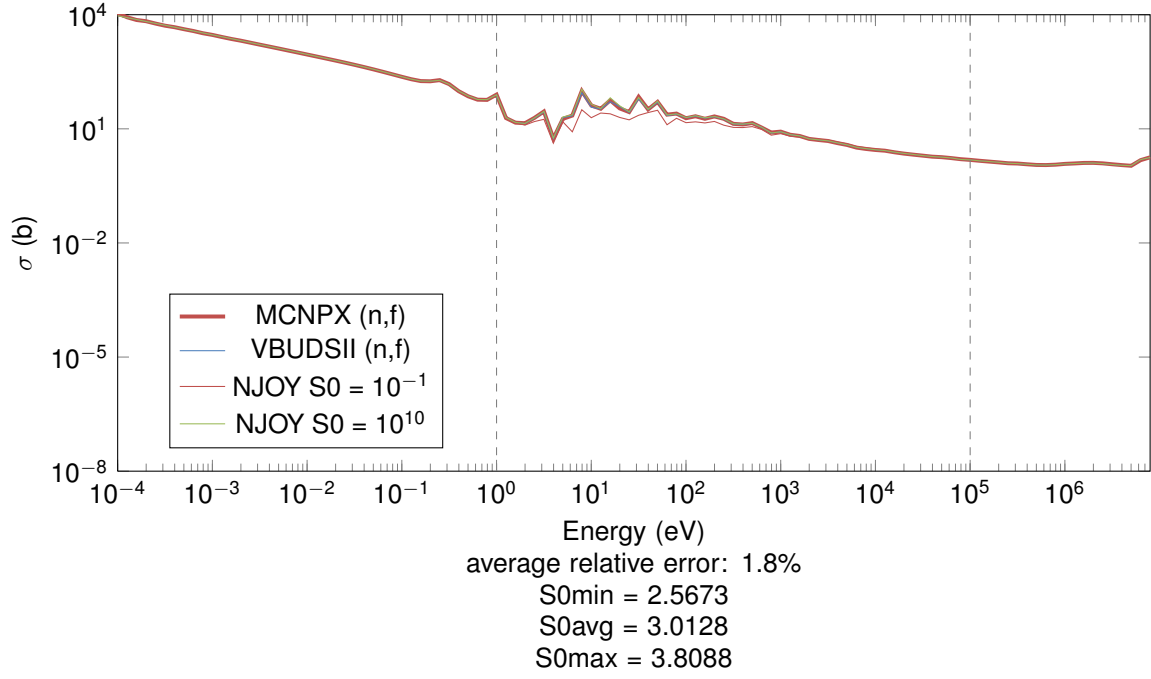


Figure 14: Energy-dependent cross sections in the UO2 cell for ZAIID 92235 and MT 18, generated by both MCNPX and VBUDSII.

### 1.2.3 Cross sections in cell UO2, for ZAIID 92238

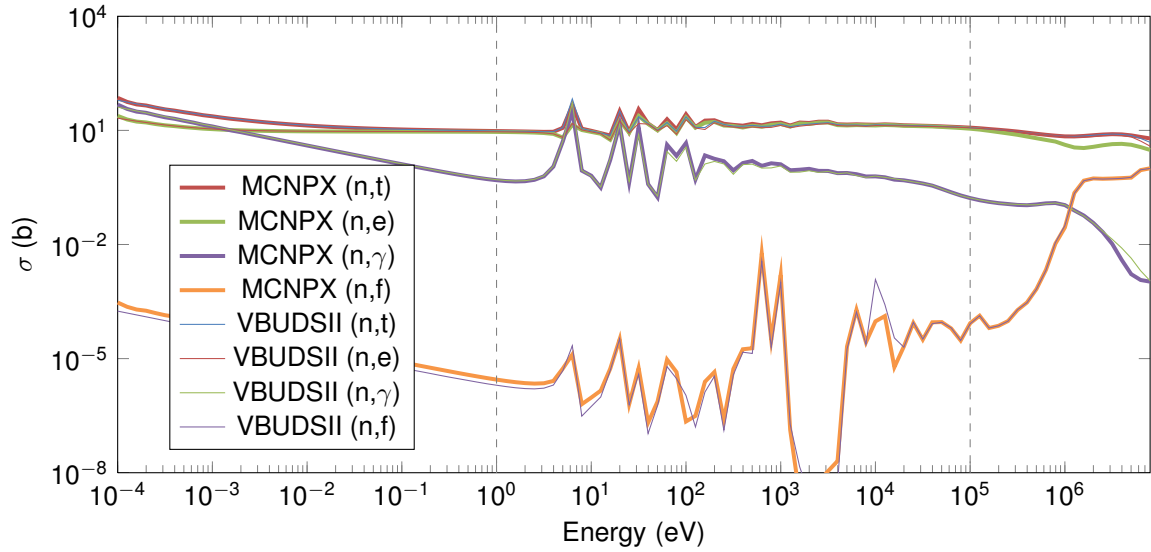


Figure 15: Energy-dependent cross sections in the UO2 cell for ZAIID 92238, generated by both MCNPX and VBUDSII.



### 1.2.4 Cross sections in cell UO2, for Z Aid 92238, separated by reaction type

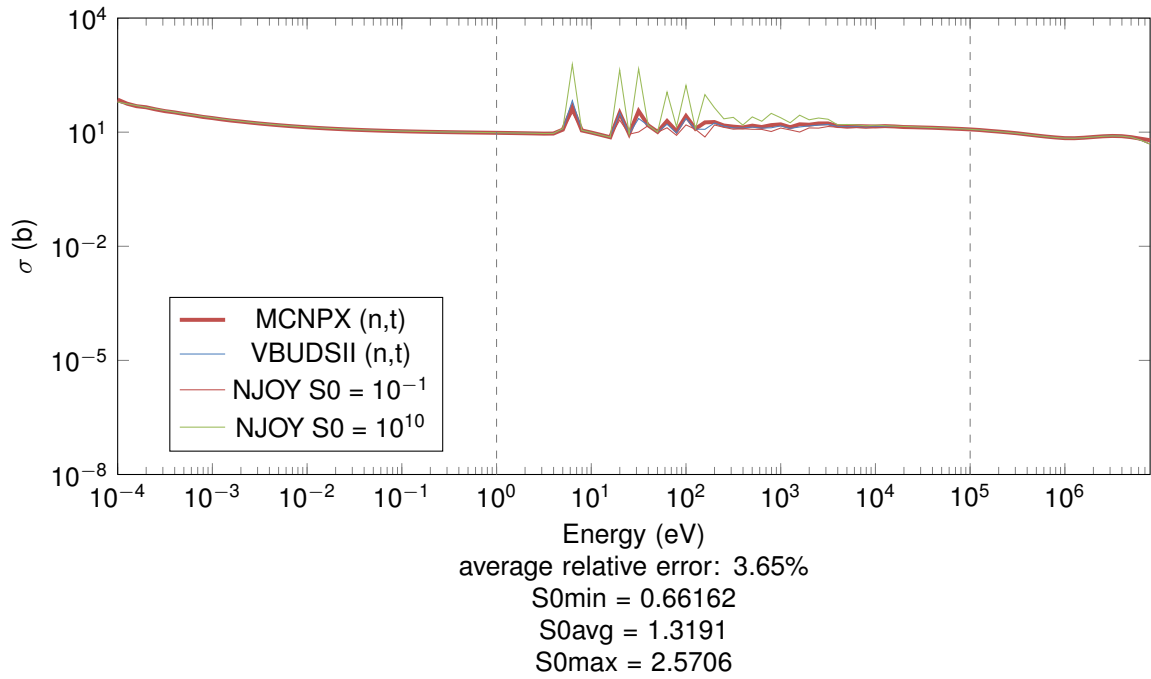


Figure 16: Energy-dependent cross sections in the UO2 cell for Z Aid 92238 and MT 7, generated by both MCNPX and VBUDSII.

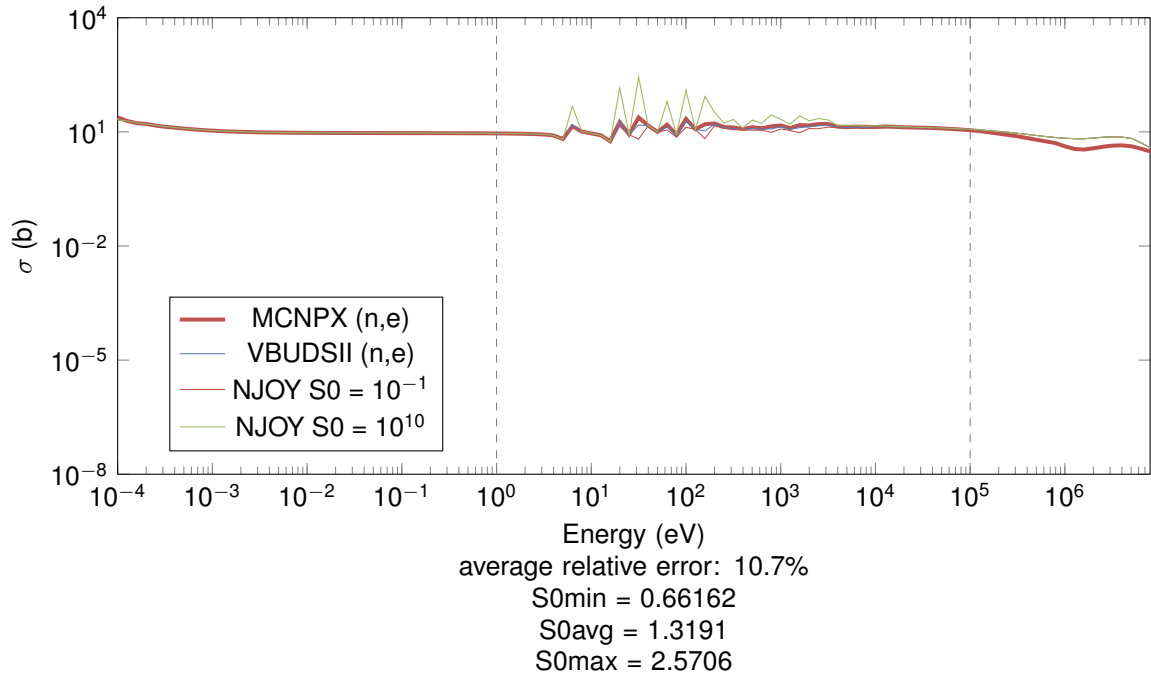


Figure 17: Energy-dependent cross sections in the UO2 cell for Z Aid 92238 and MT 2, generated by both MCNPX and VBUDSII.

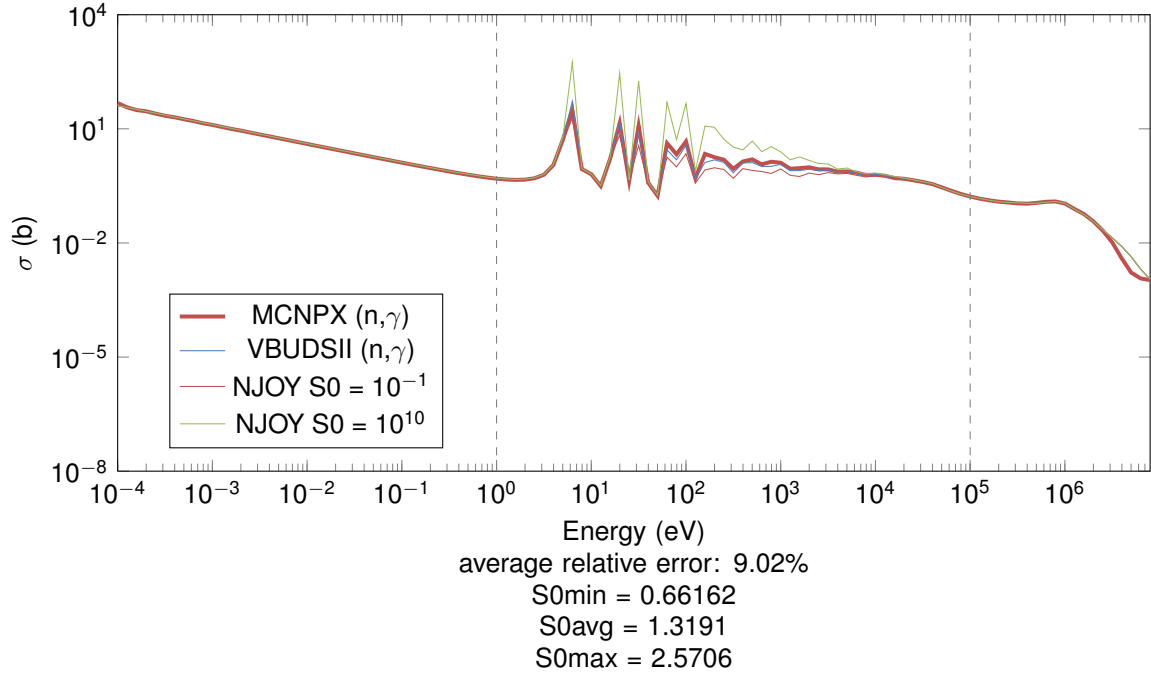


Figure 18: Energy-dependent cross sections in the UO2 cell for ZAIID 92238 and MT 102, generated by both MCNPX and VBUDSII.

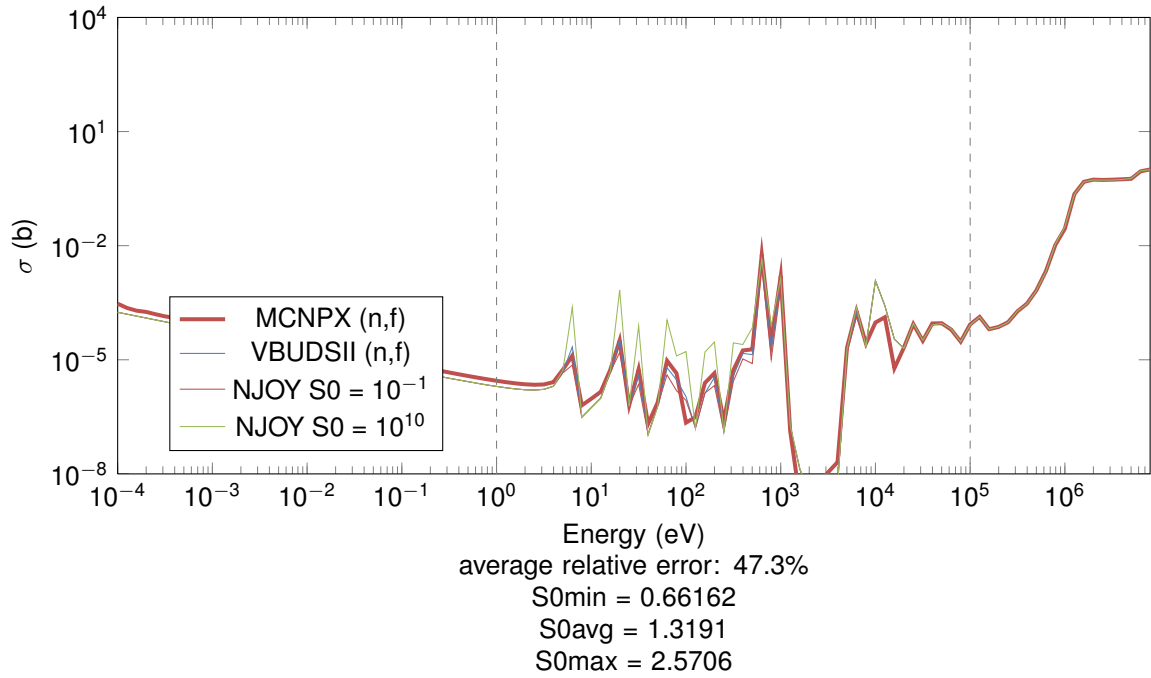


Figure 19: Energy-dependent cross sections in the UO2 cell for ZAIID 92238 and MT 18, generated by both MCNPX and VBUDSII.

### 1.2.5 Cross sections in cell UO2, for ZAID 8016

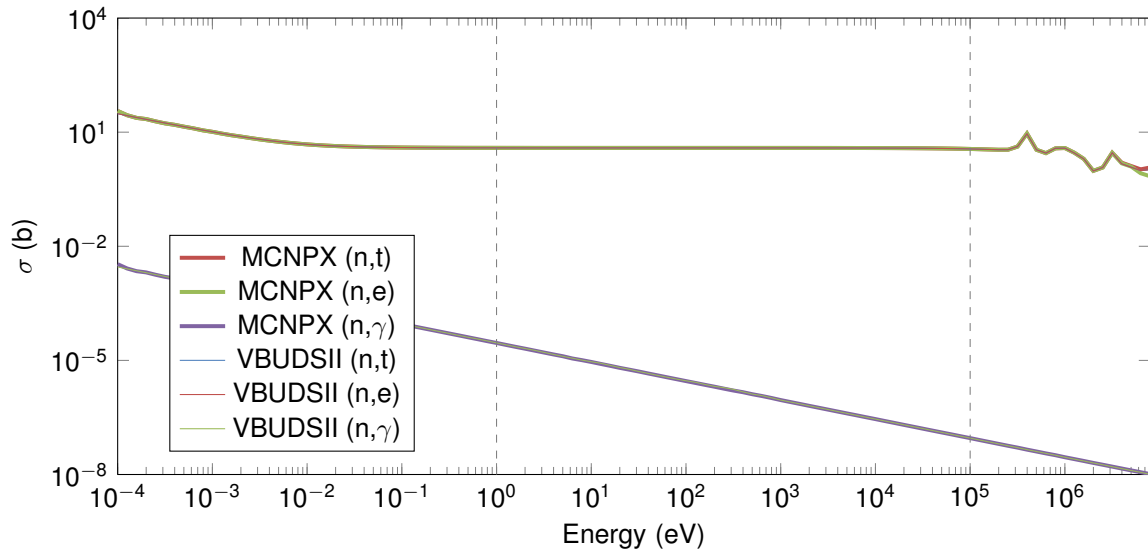


Figure 20: Energy-dependent cross sections in the UO2 cell for ZAID 8016, generated by both MCNPX and VBUDSII.

### 1.2.6 Cross sections in cell UO2, for ZAID 8016, separated by reaction type

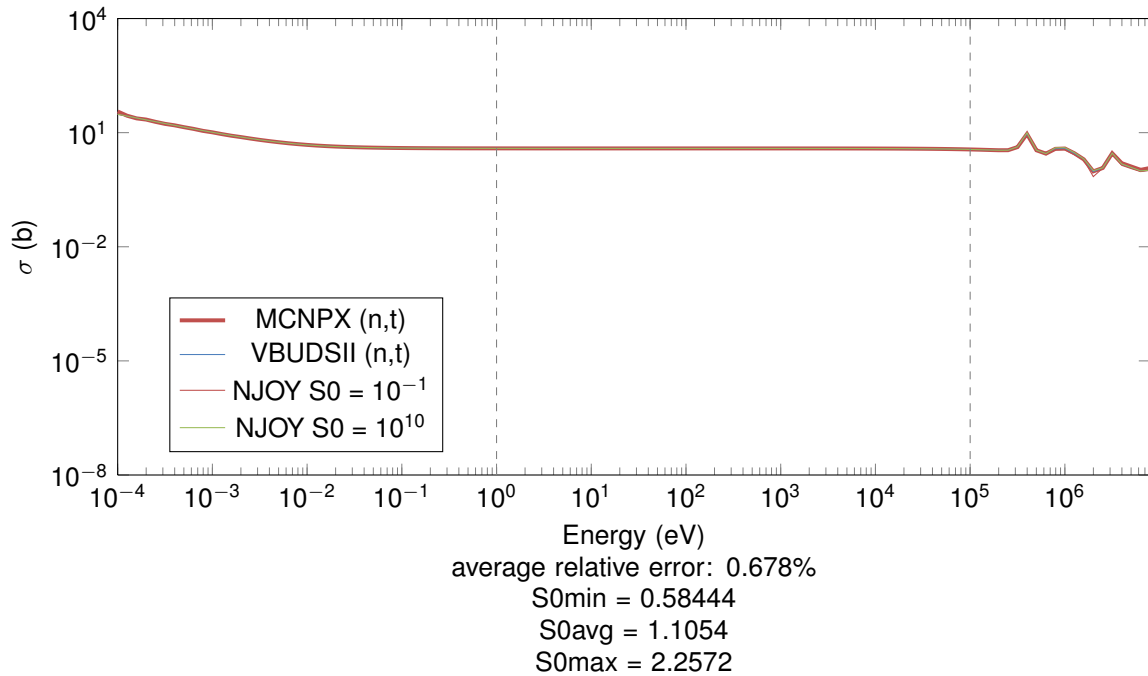


Figure 21: Energy-dependent cross sections in the UO2 cell for ZAID 8016 and MT 7, generated by both MCNPX and VBUDSII.

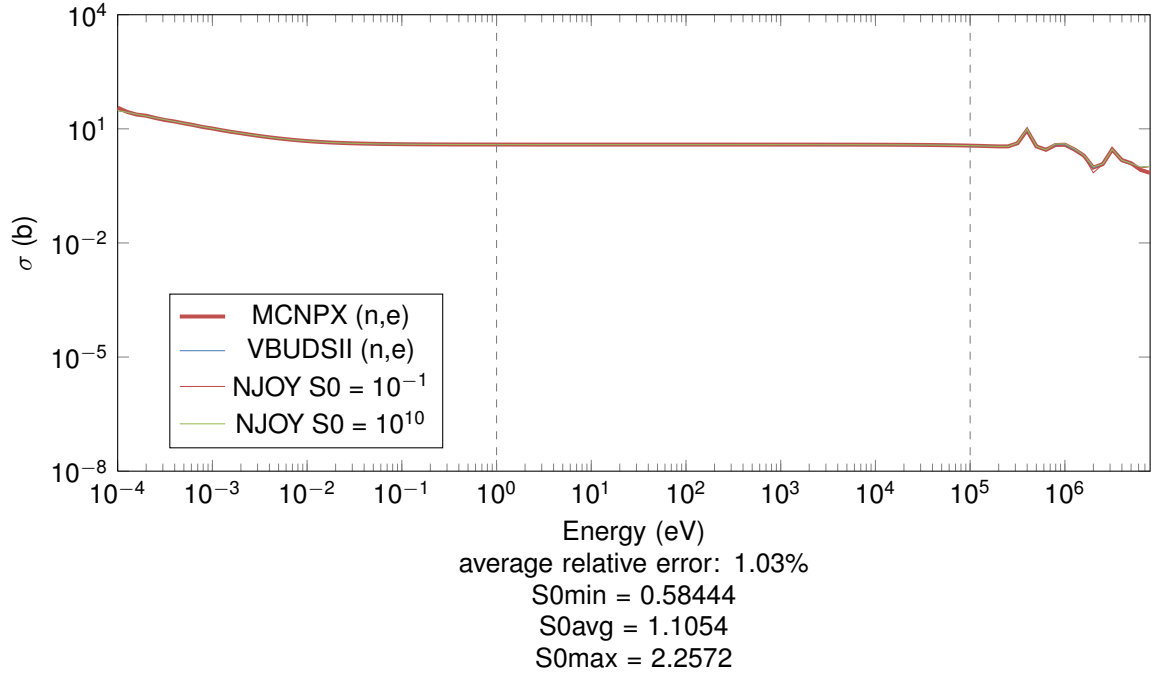


Figure 22: Energy-dependent cross sections in the UO2 cell for ZAIID 8016 and MT 2, generated by both MCNPX and VBUDSII.

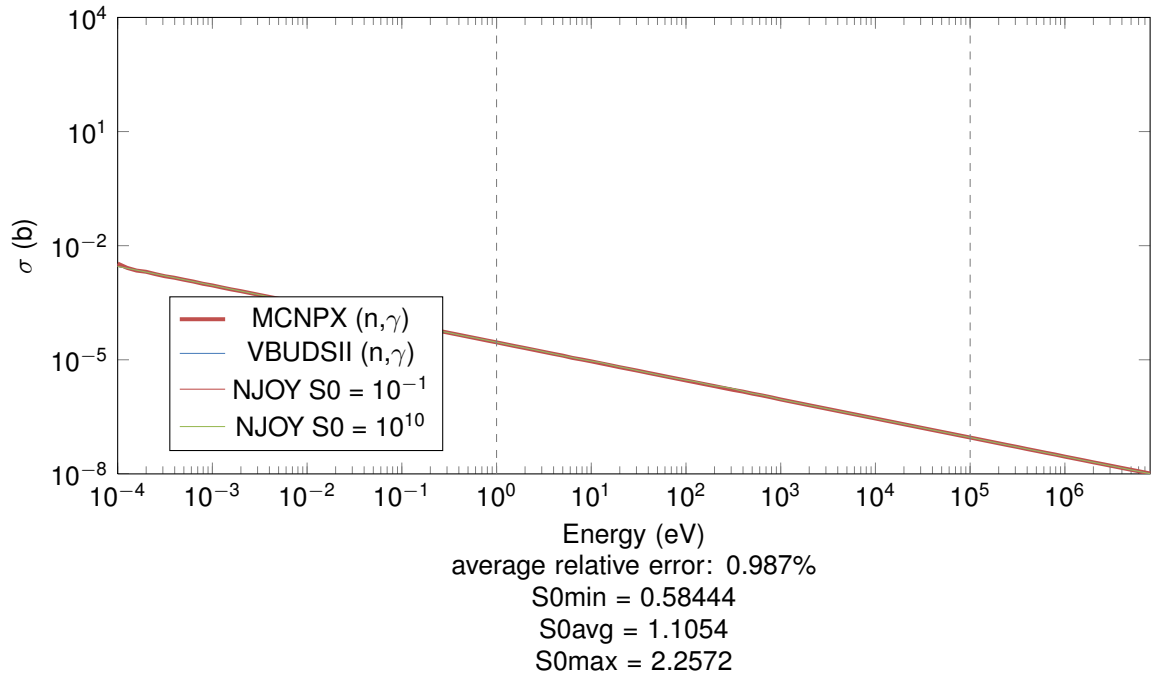


Figure 23: Energy-dependent cross sections in the UO2 cell for ZAIID 8016 and MT 102, generated by both MCNPX and VBUDSII.

MT 7: total

MT 4: inelastic scattering  
MT 2: elastic scattering  
MT 102: radiative capture  
MT 18: fission  
XS error 1: `nanmean(abs(V-M) ./M)`  
XS error 2: `V'*M/norm(V)/norm(M)`  
XS error 3: `log10(V) '*log10(M)/norm(log10(V))/norm(log10(M))`

cell	ZAID	MT	XS error 1	XS error 2	XS error 3	VBUDSII RR	MCNPX RR	RR error
1	222	7	1.3	NaN	NaN	4.8	2.2	1.18
1	222	2	1.3	NaN	NaN	4.79	2.2	1.18
1	222	102	0.9	NaN	NaN	$9.91 \cdot 10^{-3}$	$5.63 \cdot 10^{-3}$	0.76
2	92,235	7	$1.73 \cdot 10^{-2}$	NaN	NaN	10.27	11.2	$8.3 \cdot 10^{-2}$
2	92,235	2	$7.38 \cdot 10^{-2}$	NaN	NaN	1.1	1.2	$7.99 \cdot 10^{-2}$
2	92,235	102	$2.65 \cdot 10^{-2}$	NaN	NaN	1.58	1.7	$7.51 \cdot 10^{-2}$
2	92,235	18	$1.8 \cdot 10^{-2}$	NaN	NaN	7.6	8.2	$7.39 \cdot 10^{-2}$
2	92,238	7	$3.65 \cdot 10^{-2}$	NaN	NaN	1.15	1.39	0.17
2	92,238	2	0.11	NaN	NaN	1.04	1.14	$8.5 \cdot 10^{-2}$
2	92,238	102	$9.02 \cdot 10^{-2}$	NaN	NaN	0.11	0.12	$6.25 \cdot 10^{-2}$
2	92,238	18	0.47	NaN	NaN	$6.35 \cdot 10^{-3}$	$1.23 \cdot 10^{-2}$	0.48
2	8,016	7	$6.78 \cdot 10^{-3}$	NaN	NaN	0.38	0.45	0.16
2	8,016	2	$1.03 \cdot 10^{-2}$	NaN	NaN	0.38	0.45	0.16
2	8,016	102	$9.87 \cdot 10^{-3}$	NaN	NaN	$2.64 \cdot 10^{-6}$	$2.86 \cdot 10^{-6}$	$7.67 \cdot 10^{-2}$